A Data-Driven Deep Learning Network for Massive MIMO Detection with High-order QAM

Yongzhi Yu, Jie Ying, Ping Wang, and Limin Guo

***Abstract*—Massive multiple-input multiple-output (MIMO) can provide higher spectral efficiency and energy efficiency compared to conventional MIMO systems. Unfortunately, as the numbers of modulation orders and antennas increase, the computational complexity of conventional symbol detection algorithms becomes unaffordable and their performance deteriorates. However, deep learning (DL) techniques can provide flexibility, nonlinearity and computational parallelism for massive MIMO detection to address these challenges. We propose an efficient data-driven detection network, i.e., accelerated multiuser interference cancellation network (AMIC-Net), for uplink massive MIMO systems. Specifically, we first introduce an extrapolation factor regarded as a learnable parameter into the multiuser interference cancellation (MIC) algorithm for iterative sequential detection (ISD) detector through extrapolation technique to enhance the convergence performance. Then we unfold the above accelerated iterative algorithm and adopt a sparsely connected approach, instead of fully connected, to obtain a relatively simple deep neural network (DNN) structure to enhance the detection performance through the data-driven DL approach. Furthermore, in order to accommodate communication scenarios with higher-order modulation, a novel activation function is proposed, which is composed of multiple softsign activation functions with additional learnable parameters to implement a multi-segment mapping of the set of constellation points with different modulations. Numerical results show that the proposed DL network can bring significant performance gain to ISD detector with various massive antenna settings and outperform the existing detectors with the same or lower computational complexity, especially in high-order QAM modulation scenarios.**

***Index Terms*—Data-driven detection network, deep learning, high-order QAM modulation, massive MIMO detection, multiuser interference cancellation.**

I. Introduction

MASSIVE multiple-input multiple-output (MIMO), which can significantly improve spectral efficiency and energy efficiency, is one of the most promising technologies for fifth generation mobile communications (5G) [1], machine-to-machine communications (M2M) [2], [3] and other wireless communication systems. And its large number of antennas (e.g., tens or hundreds of antennas) at the subscribers and base stations (BS) endow the system to achieve high speed and low latency transmission [4], [5]. However, such large-scale deployments also pose significant difficulties for MIMO detection. The problem statement for MIMO detection is simple - to infer the original transmitted signal from the signal received at the BS antennas. But how to build a MIMO detector that can achieve high detection accuracy with low complexity is a challenging research problem, especially for massive MIMO deployments.

It is well known that the maximum likelihood (ML) detector [6] is optimal but with the highest computational complexity due to the consideration of all possible combinations of transmit symbols. Therefore, some linear detectors such as the zero forcing (ZF) [7] detector and the linear minimum mean squared error (MMSE) [7] detector are proposed to reduce the computational complexity, but they require the inverse of the matrix to obtain the estimated signal, which is very complicated in massive MIMO scenarios. Also, some other suboptimal algorithms, e.g., the sphere decoding (SD) [8], semidefinite relaxation (SDR) [9], approximate message passing (AMP) [10] and orthogonal AMP (OAMP) [11], have been validated the near-optimal performance in some case. However, they suffer from severe degradation in detection accuracy and dramatic increase in complexity when the number of antennas is incremented.

As one of the most efficient and promising core technologies to artificial intelligence, deep learning (DL) has achieved tremendous success in many fields, such as computer vision, natural language processing and wireless communications [12]. Owing to its ability to achieve approximation of complex functions through nonlinear operations and neural networks, it has also recently been applied to massive MIMO signal detection in pursuit of enhanced performance. In fact, the deep learning approaches for MIMO signal detection are classified into two main categories, namely model-driven approaches and data-driven approaches [13], [14]. Model-driven approaches are mainly to construct an iterative network by adding a few learnable parameters to the existing algorithmic model, also known as deep unfolding [13]. In [15], [16] and [17], the learned conjugate gradient descent network (LcgNet), model-driven deep learning-based (DL-based) and OAMP deep network (OAMP-Net) are deep unfolding of the conjugate gradient descent algorithm [18], multiuser interference cancellation (MIC) algorithm [19] and OAMP algorithm [11], respectively. By learning the optimal parameters from the training data, they have been proven to outperform the original algorithms and are trained quickly due to the minimal

Manuscript received June 14, 2022; revised October 8, 2022; approved for publication by Zhao Jun, Division 2 Editor, November 12, 2022. This work was supported by the Fundamental Research Funds for the Central Universities (Grant Number: 3072022CF0802).

Y. Yu, J. Ying and L. Guo are with the College of Information and Communication Engineering, Harbin Engineering University, Harbin 150001, China, email: yuyongzhi@hrbeu.edu.cn; hwfsmp@163.com; guolimin22@163.com.

P. Wang is with the Department of Electrical Engineering and Computer Science, York University, Toronto, ON M3J 1P3, Canada, email: ping.wang@lassonde.yorku.ca.

Digital Object Identifier: 10.23919/JCN.2022.000055

1229-2370/22/$10.00 © 2022 KICS

number of learnable parameters. But unfortunately, as these algorithmic models are with a low level of nonlinearity and few learnable parameters, their performance is limited by the original algorithmic structure, resulting in limited performance gains or difficulty in handling the complex situation of massive MIMO [15]. Data-driven approaches, on the other hand, learn features directly from large amounts of data without relying on relevant models for problem solution. The detection network (DetNet), as a paradigm of data-driven approaches, is proposed in [20], [21] by unfolding a projected gradient descent algorithm to a fully connected deep neural network (DNN) network. Since DNN possesses a strong learning ability from the data and nonlinear expression, the DetNet achieves a comparable performance to those of the SDR and AMP detectors at the expense of heavy training time. Then, an improved network proposed in [22], the sparsely connected neural network (ScNet), is obtained mainly by simplifying the connection structure of the DetNet, which tremendously reduces the network complexity and training time consumption. Furthermore, in order to improve the detection performance of the ScNet in high-order modulation scenarios, the multi-segment mapping network (MsNet), which builds a staircase function based on the sigmoid activation function, is introduced in [23]. The results of these studies demonstrate unprecedented performance improvement thanks to the DNN framework. In contrast to model-driven, the DNN network designed by the data-driven approach exhibits a higher level of nonlinearity and flexibility attributed to deeper network layers and a sufficient number of learnable parameters, which can solve much harder and larger problems to achieve better results at the cost of memory space due to the increase in the model parameters [24].

In this work, motivated by these findings, we propose a data-driven DL network, namely the AMIC-Net, for uplink massive MIMO detection. Furthermore, in order to accommodate communication scenarios with higher-order modulation, we devise a novel activation function that implements a multi-segment mapping of the set of constellation points with different modulations. Our contributions are summarized below:

- First, an extrapolation factor is introduced into the multiuser interference cancellation (MIC) algorithm [19] and treated as a learnable parameter to enhance the convergence speed and robustness. Then our proposed DL network is derived by unfolding the above accelerated MIC (AMIC) algorithm and adopting a sparsely connected approach instead of fully connected to obtain a relatively simple DNN structure to achieve promising improvement in detection accuracy through the data-driven DL approach.
- A novel activation function, referred to as the SoftS function, is designed to improve detection performance under high-order modulation, which is composed of multiple softsign activation functions with additional learnable parameters. Its curve is flatter and the gradient is non-zero everywhere compared to the sigmoid function. This appealing property allows the AMIC-Net to learn more efficiently through backward propagation and prevents gradient vanishing due to the saturation of the activation functions. The simulation results show that our designed activation function is far superior to other activation functions in the case of complex high-order modulation.
- The detection performance and computational complexity comparison of the AMIC-Net with other reported detectors, including data-driven approaches, model-driven approaches and traditional algorithms, are given. Our study and results show that the proposed AMIC-Net has almost the same detection accuracy as OAMP-Net, but with at least 10 times lower computational complexity. Furthermore, AMIC-Net brings significant performance gain to ISD detector with various massive antenna settings and outperforms the existing detectors with the same or lower computational complexity, especially in high-order QAM modulation scenarios.

Notations: Throughout the entire paper, scalars, vectors and matrices are respectively denoted by lowercase, boldface lowercase, and boldface uppercase letters. $\Re(\cdot)$ and $\Im(\cdot)$ denote the real and imaginary parts of a complex vector or matrix. $(\cdot)^T$ and $(\cdot)^{-1}$ denote the transpose and matrix inversion, respectively. $\mathbf{I}_N$ represents the N dimensional identity matrix. The symbol $\odot$ denotes the Hadamard product. $\|\cdot\|$ denotes the Euclidean norm of a vector or matrix. $\mathrm{sign}(\cdot)$ is used to represent the signum function, where $\mathrm{sign}(x) = 1$ when $x \geq 0$, and $\mathrm{sign}(x) = -1$ otherwise.

II. Preliminaries on Massive MIMO Detection

A. System Model

We consider the uplink massive MIMO system with M antennas at the base station (BS) and K single-antenna users. The transmitted signal vector $\tilde{\mathbf{s}} \in \mathbb{C}^{K\times 1}$ from the users is transmitted to the BS through the Rayleigh fading channel $\tilde{\mathbf{H}} \in \mathbb{C}^{M\times K}$. The received signal vector $\tilde{\mathbf{y}} \in \mathbb{C}^{M\times 1}$ at the BS is given by

$$\tilde{\mathbf{y}} = \tilde{\mathbf{H}}\tilde{\mathbf{s}} + \tilde{\mathbf{n}}, \tag{1}$$

where $\tilde{\mathbf{n}} \in \mathbb{C}^{M\times 1}$ is the additive white Gaussian noise (AWGN) vector with zero mean and variance σ^2.

For easy handling in DL, we can convert the complex model (1) to an equivalent real one as

$$\mathbf{y} = \mathbf{H}\mathbf{s} + \mathbf{n}, \tag{2}$$

where

$$\begin{aligned} \mathbf{y} &= \begin{bmatrix} \Re(\tilde{\mathbf{y}}) \\ \Im(\tilde{\mathbf{y}}) \end{bmatrix} \in \mathbb{R}^{2M\times 1}, \boldsymbol{s} = \begin{bmatrix} \Re(\tilde{\mathbf{s}}) \\ \Im(\tilde{\mathbf{s}}) \end{bmatrix} \in \mathbb{R}^{2K\times 1}, \\ \mathbf{n} &= \begin{bmatrix} \Re(\tilde{\mathbf{n}}) \\ \Im(\tilde{\mathbf{n}}) \end{bmatrix} \in \mathbb{R}^{2M\times 1}, \\ \mathbf{H} &= \begin{bmatrix} \Re(\tilde{\mathbf{H}}) & -\Im(\tilde{\mathbf{H}}) \\ \Im(\tilde{\mathbf{H}}) & \Re(\tilde{\mathbf{H}}) \end{bmatrix} \in \mathbb{R}^{2M\times 2K}. \end{aligned} \tag{3}$$

The estimated signal vector for MMSE detector can be expressed as

$$\tilde{\mathbf{s}}_{\text{MMSE}} = (\mathbf{H}^T\mathbf{H} + \frac{\sigma^2}{E_x}\mathbf{I}_{2K})^{-1}\mathbf{H}^T\mathbf{y} = \mathbf{A}^{-1}\mathbf{b}, \tag{4}$$

where E_x is the average energy per symbol, $\mathbf{A} = \mathbf{H}^T\mathbf{H} + (\sigma^2/E_x)\mathbf{I}_{2K}$ denotes the MMSE filtering

matrix, $\mathbf{b} = \mathbf{H}^T\mathbf{y}$ represents the matched-filter output of $\mathbf{y}$. Despite the relatively low complexity of the linear detector MMSE compared to ML detection, the computational complexity of $\mathbf{A}^{-1}$ is very large due to the high dimensionality of the channel matrix $\mathbf{H}$ in massive MIMO, making it difficult to implement. And when the loading factor $M/K \leq 10$, MMSE suffers a large gap in detection accuracy with the optimal ML detection [7].

B. MIC Algorithm for Iterative Sequential Detection (ISD) Detector

An iterative sequential detection (ISD) detector based on the MIC algorithm has been proposed to address the significant degradation in detection accuracy as the number of users increases by iteratively detecting transmitted symbols from each user in a sequential fashion [19].

In ISD detector, the received signal from the jth user that removes the interference from other users can be written as

$$\hat{\mathbf{y}}_j = \mathbf{y} - \sum_{k=1,k\neq j}^{2K} \mathbf{h}_k \hat{s}^l(k) = \mathbf{h}_j \hat{s}^{l+1}(j), \tag{5}$$

where l denotes the iteration index, $\mathbf{h}_j$ is the jth column of $\mathbf{H}$, and $\hat{s}^{l+1}(j)$ is the jth element of the $\hat{\mathbf{s}}^{l+1} = [\hat{s}^{l+1}(1), \hat{s}^{l+1}(2), \cdots, \hat{s}^{l+1}(2K)]^T$, $j = 1, \cdots, 2K$.

To detect $\hat{s}^{l+1}(j)$, it can be deduced as

$$\begin{aligned}
\hat{s}^{l+1}(j) &= \frac{\mathbf{h}_j^T}{\|\mathbf{h}_j\|^2}\hat{\mathbf{y}}_j \\
&= \frac{1}{\|\mathbf{h}_j\|^2}\left(\mathbf{h}_j^T\mathbf{y} - \mathbf{h}_j^T\sum_{k=1,k\neq j}^{2K}\mathbf{h}_k\hat{s}^l(k)\right) \\
&= \frac{1}{\|\mathbf{h}_j\|^2}\left(\mathbf{h}_j^T\mathbf{y} - \mathbf{h}_j^T\sum_{k=1}^{2K}\mathbf{h}_k\hat{s}^l(k)\right) + \frac{\mathbf{h}_j^T\mathbf{h}_j}{\|\mathbf{h}_j\|^2}\hat{s}^l(j) \\
&= \frac{1}{\|\mathbf{h}_j\|^2}\left(\mathbf{h}_j^T\mathbf{y} - \mathbf{h}_j^T\sum_{k=1}^{2K}\mathbf{h}_k\hat{s}^l(k)\right) + \hat{s}^l(j)
\end{aligned} \tag{6}$$

Let diagonal matrix $\mathbf{D} = diag(\mathbf{H}^T\mathbf{H}) = diag\{d_1, d_2, \cdots, d_j, \cdots, d_k\}$, where $d_j = \|\mathbf{h}_j\|^2$. Then, (6) can be expressed as

$$\hat{s}^{l+1}(j) = \hat{s}^l(j) + \frac{1}{d_j}\left(\mathbf{h}_j^T\mathbf{y} - \sum_{k=1}^{2K}(\mathbf{H}^T\mathbf{H})_{j,k}\hat{s}^l(k)\right). \tag{7}$$

Further, (7) can be rewritten in matrix-vector form as

$$\hat{\mathbf{s}}^{l+1} = \hat{\mathbf{s}}^l + \mathbf{D}^{-1}(\mathbf{H}^T\mathbf{y} - \mathbf{H}^T\mathbf{H}\hat{\mathbf{s}}^l). \tag{8}$$

III. Proposed Data-Driven AMIC-Net

In this section, we first present a data-driven AMIC-Net for massive MIMO detection, and detail the structure of AMIC-Net. Afterwards, we design a novel activation function for the high-order modulation scenario. Since (8) is a recursive iterative algorithm, an extrapolation factor is introduced into the structure of (8) to improve the convergence performance by using an extrapolation technique [22], which is formulated as follows:

$$\begin{aligned}
\hat{\mathbf{s}}^{l+1} &= \gamma(\hat{\mathbf{s}}^l + \mathbf{D}^{-1}(\mathbf{H}^T\mathbf{y} - \mathbf{H}^T\mathbf{H}\hat{\mathbf{s}}^l)) + (1-\gamma)\hat{\mathbf{s}}^l \\
&= \hat{\mathbf{s}}^l + \gamma\mathbf{D}^{-1}(\mathbf{H}^T\mathbf{y} - \mathbf{H}^T\mathbf{H}\hat{\mathbf{s}}^l),
\end{aligned} \tag{9}$$

where γ is the optimum extrapolation factor, which can be exactly calculated as [25]

$$\gamma = \frac{2}{\lambda_{min} + \lambda_{max}}, \tag{10}$$

where λ_{min} and λ_{max} are the minimum and maximum eigenvalue of $\mathbf{D}^{-1}\mathbf{H}^T\mathbf{H}$. We replace the calculations of γ,which originally involves matrix eigenvalue operations, with a learnable parameter that can be trained by DL to obtain an appropriate extrapolation factor, which not only reduces the computation complexities, but also enhances the robustness of convergence. Thus, (9) can be represented by

$$\hat{\mathbf{s}}^{l+1} = \hat{\mathbf{s}}^l + \beta\mathbf{D}^{-1}(\mathbf{H}^T\mathbf{y} - \mathbf{H}^T\mathbf{H}\hat{\mathbf{s}}^l), \tag{11}$$

where β is a learnable parameter.

Data-driven DL approaches, one of the most popular methods for building neural networks, can demonstrate a better performance than traditional algorithms in many cases and has potential to handle more complex situations due to their powerful learning capabilities and nonlinear expression. Motivated by this idea, we propose a DNN network, namely AMIC-Net, by unrolling the iterations of (11) to get a performance boost. It is evident from (11) that each iteration is just related to $\hat{\mathbf{s}}^l$ and $\beta\mathbf{D}^{-1}(\mathbf{H}^T\mathbf{y} - \mathbf{H}^T\mathbf{H}\hat{\mathbf{s}}^l)$, so we concatenate them into a single vector as the input of AMIC-Net to raise the input dimension for the construction of DNN network with a large number of nodes.

In addition, since only the elements between $\hat{\mathbf{s}}^l$ and $\beta\mathbf{D}^{-1}(\mathbf{H}^T\mathbf{y} - \mathbf{H}^T\mathbf{H}\hat{\mathbf{s}}^l)$ vectors are linearly added or subtracted at the same index, there is no relationship with the other elements of these vectors. Therefore, utilizing this feature, the AMIC-Net we proposed employs sparse connections in the neural network similar to ScNet [22] instead of full connections. By cutting out meaningless connections, only meaningful connections can be formed to ensure the efficiency of the network and maximize its working capacity. It is worth noting that this can effectively reduce the complexity of the network and enhance the detection performance to some extent. Then, the architecture of the network is as follows:

$$\hat{\mathbf{s}}^{l+1} = \Pi\left(\mathbf{P}\odot\mathbf{W}^l\begin{bmatrix}\hat{\mathbf{s}}^l \\ \beta^l\mathbf{D}^{-1}(\mathbf{H}^T\mathbf{y} - \mathbf{H}^T\mathbf{H}\hat{\mathbf{s}}^l)\end{bmatrix} + \mathbf{b}^l\right), \tag{12}$$

where $\Pi(\cdot)$ represents a nonlinear operator to enhance the expression of the network, $\mathbf{W}^l$ and $\mathbf{b}^l$ are the weight matrix of $2K\times 4K$ dimension and the bias vector of $2K\times 1$ dimension, respectively, $\mathbf{P}$ is a weight connection matrix of $\mathbf{W}^l$ used to generate the sparsity.

The structure of the AMIC-Net is illustrated in Fig. 1, which is built based on the MIC algorithm. The input of the AMIC-Net is $\mathbf{H}^T\mathbf{H}$, $\mathbf{H}^T\mathbf{y}$, $\mathbf{D}^{-1}$ and the initial estimate $\hat{\mathbf{s}}^0$, while the output is the final estimate $\hat{\mathbf{s}}^L$ of the transmitted signal $\hat{\mathbf{s}}$. Moreover, the network is composed of L cascade layers and

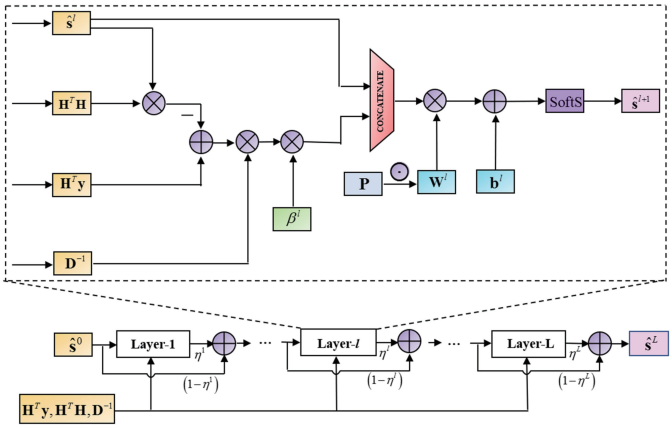

Fig. 1. The structure of the proposed AMIC-Net.

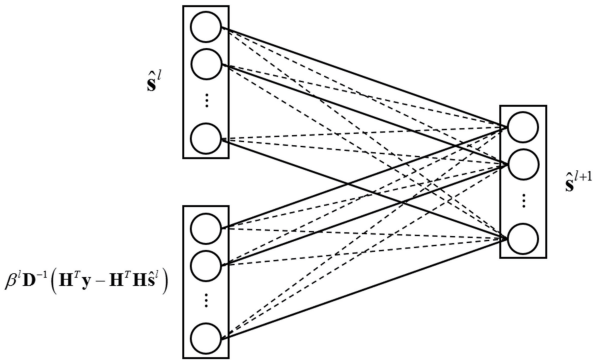

Fig. 2. Neural network connection for AMIC-Net.

each layer has the same structure but with different parameter values. For the lth layer of the AMIC-Net, the input $\hat{\mathbf{s}}^l$ is the estimated signal from the $(l-1)$th layer, and the output $\hat{\mathbf{s}}^{l+1}$ is also input of the next layer. The SoftS function is the staircase activation function to be designed later in this work. Further, the weight connection matrix $\mathbf{P}$ is a sparse matrix, when $K=2$, it can be expressed as

$$\begin{aligned}\mathbf{P} &= \begin{bmatrix} 1 & 0 & 0 & 0 & 1 & 0 & 0 & 0 \\ 0 & 1 & 0 & 0 & 0 & 1 & 0 & 0 \\ 0 & 0 & 1 & 0 & 0 & 0 & 1 & 0 \\ 0 & 0 & 0 & 1 & 0 & 0 & 0 & 1 \end{bmatrix} \\ &= [\mathbf{I}_{2K} \quad \mathbf{I}_{2K}].\end{aligned} \tag{13}$$

From (13), it can be seen that the weight connection matrix $\mathbf{P}$ consists of two identity matrices of $2K$ dimension, which controls the sparsity of the weights of each layer, leading to a sparse connection between adjacent layers. The neural network connections represented in the form of nodes are shown in Fig. 2, where each node denotes one of the elements of the vector. As can be seen in Fig. 2, the solid line connection between each node of the output and the input at the same index is represented by 1 in the weight connection matrix $\mathbf{P}$, while the dashed line connection between the input and output nodes at different indexes is represented by 0 in the $\mathbf{P}$ matrix, which indicates that no information exchange is required, thereby yielding sparsity.

To accommodate communication scenarios with high-order

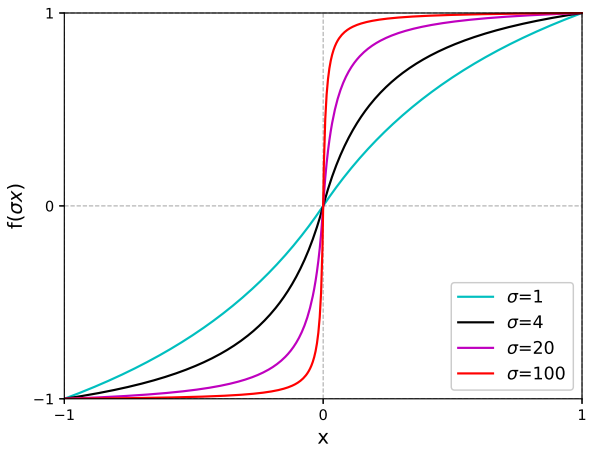

Fig. 3. $f(\sigma x)$ with different slope σ.

QAM modulation, an ingenious approach is to build a staircase function consisting of a universal activation function to perform multi-segment mapping of the input, such as $\psi_t(\cdot)$ for DetNet [21] and sigS$(\cdot)$ for MsNet [23]. sigS$(\cdot)$ solves the problem that $\psi_t(\cdot)$ is not derivable at the inflection point, however, it is designed based on a sigmoid function with saturation at both ends, which prevents the backward propagation of the gradients during the training process, leading to unexpected performance losses of the network. Thus, in order to overcome these difficulties, we designed a new staircase function, referred to as SoftS$(\cdot)$, in $\Pi(\cdot)$ to implement a multi-segment mapping of the input in different modulation modes. The SoftS$(\cdot)$ is based on the following softsign$(\cdot)$ activation function:

$$\text{softsign}(x) = \frac{x}{1+|x|}. \tag{14}$$

In order for the softsign(σx) function to have a range of $[-1,1]$ when the domain of definition is $[-1,1]$, we stretch it vertically as follows:

$$f(\sigma x) = (1+\frac{1}{\sigma})\text{softsign}(\sigma x), \tag{15}$$

where σ can be interpreted as the slope. Fig. 3 shows the curves of $f(\sigma x)$ with different values of σ. It can be observed that if the slope is too large, the curve will tend to saturate at both ends with zero gradient, whereas if the slope is too small, it will cause the output to oscillate. Thus, on balance, we take $\sigma = 4$.

Our proposed staircase function is made of multiple

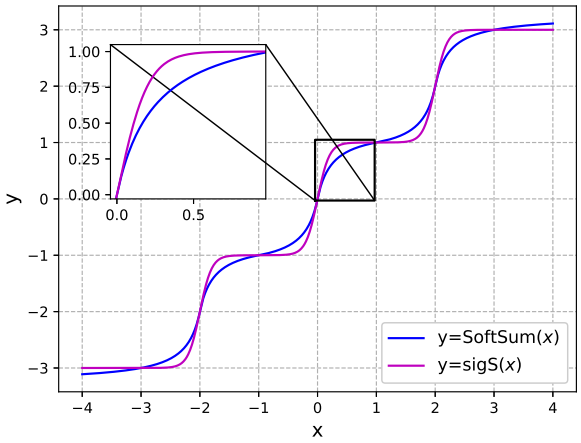

Fig. 4. SoftSum and sigS function mapping curve under 16-QAM modulation.

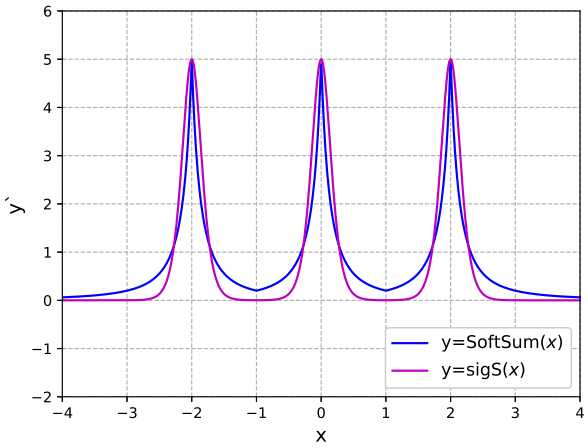

Fig. 5. SoftSum and sigS function derivative curve under 16-QAM modulation.

softsign$(\cdot)$ functions with different offsets, which is given by

$$\begin{aligned}&\text{SoftSum}(x)\\&=\sum_{t=1}^{2N-3}\left(\frac{\text{sign}(x+1+G_t)-\text{sign}(x-1+G_t)}{2}\right.\\&\left.\times((1+\frac{1}{4})\text{softsign}(4(x+G_t))-G_t)\right)\\&+\sum_{t=2N-2}^{2N-1}\left(\frac{1-(-1)^t\text{sign}(x-1+G_t)}{2}\right.\\&\left.\times((1+\frac{1}{4})\text{softsign}(4(x+G_t))-G_t)\right).\end{aligned}\tag{16}$$

$$G_t=\frac{1}{2}+(-1)^t(t-\frac{1}{2}),\tag{17}$$

where $\text{sign}(\cdot)$ is a signum function applied to restrict the domain of definition of the softsign$(\cdot)$ function, and G_t is the step size of the translation, and $2N$ $(2N\geq 4)$ is the sum of constellation points sets in high-order QAM modulation. Figs. 4 and 5 show the mapping curves and derivative curves of SoftSum$(\cdot)$ function and sigS$(\cdot)$ function under 16-QAM modulation, respectively. It can be noted that the SoftSum$(\cdot)$ function is non-saturated and has a flatter curve compared to sigS$(\cdot)$, which means that the AMIC-Net can not only prevent the gradient from vanishing due to the saturation of the activation function but also learn more efficiently through backward propagation.

Besides, in order to allow the proposed staircase function to fine-tune its own shape according to the change in the input value of the activation function at each layer to better match the network, a set of learnable parameters $\{\theta_t^l\}_{t=1}^{2N-1}$ are introduced to (16), which is as follows:

$$\begin{aligned}&\text{SoftS}(x)\\&=\sum_{t=1}^{2N-3}\left(\frac{\text{sign}(x+1+G_t)-\text{sign}(x-1+G_t)}{2}\right.\\&\left.\times((1+\frac{1}{4\theta_t^l})\text{softsign}(4\theta_t^l(x+G_t))-G_t)\right)\\&+\sum_{t=2N-2}^{2N-1}\left(\frac{1-(-1)^t\text{sign}(x-1+G_t)}{2}\right.\\&\left.\times((1+\frac{1}{4\theta_t^l})\text{softsign}(4\theta_t^l(x+G_t))-G_t)\right).\end{aligned}\tag{18}$$

SoftS$(\cdot)$ is the final form of our activation function design.

In order to further improve the performance of the proposed network, we add the residual structure [23] as follows:

$$\hat{\mathbf{s}}^{l+1}=\eta^l\hat{\mathbf{s}}^{l+1}+(1-\eta^l)\hat{\mathbf{s}}^l,\tag{19}$$

where η^l is a learnable residual coefficient of the lth layer. The entire network structure is shown in Fig. 1.

In addition, to facilitate the convergence of the network, we sacrifice a little extra negligible computational complexity to obtain a rough MMSE estimate as an initial solution by utilizing the diagonally dominant property of $\mathbf{A}$ [26]. Then the initial solution can be expressed as

$$\hat{\mathbf{s}}^0=\mathbf{D}_\mathbf{A}^{-1}\mathbf{b},\tag{20}$$

where diagonal matrix $\mathbf{D}_\mathbf{A}$ is the diagonal component of $\mathbf{A}$. Obviously, the computational complexity of $\mathbf{D}_\mathbf{A}^{-1}$ is very low.

Moreover, we adopt the following Loss function to evaluate the distance between the outputs of all layers and the transmitted signal [22]:

$$L(\mathbf{s},\hat{\mathbf{s}})=\sum_{l=1}^{L}\log(l)\|\mathbf{s}-\hat{\mathbf{s}}^l\|^2.\tag{21}$$

TABLE I
SIMULATION SETTINGS OF AMIC-NET.

Parameters	Values	
$(K,\ M)$	(8, 64), (32, 64)	(16, 128), (32, 128)
Modulation	BPSK	16QAM, 64QAM
Batch size	2000	500
Number of training iterations	10000	16000
Size of training data	200000	200000
Size of testing data	20000	20000
SNRs for training	[0, 16]	
Starting learning rate	0.0001	
Optimization method	Adam optimizer	

IV. SIMULATION AND NUMERICAL RESULTS

In this section, we first experimentally demonstrate the detection performance of the proposed AMIC-Net with various activation functions. Then the detection performance comparison of the AMIC-Net with data-driven DetNet, ScNet, MsNet, model-driven DL-based, OAMP-Net, and conventional algorithms MMSE, ISD, OAMP detectors is given. Finally, the computational complexity is evaluated.

A. Simulation Setup

In our simulation, the proposed network AMIC-Net is implemented in TensorFlow 1.14.0 for Python [27]. Since the dimensionality of the algorithm model depends on the number of transmit antennas rather than the receive antennas, we fix the number of receive antennas to study the effect of different number of transmit antennas on the detection performance in scenarios with low-order modulation and high-order modulation, respectively. The detailed settings of the AMIC-Net under various system configurations are summarized in Table I.

The entire experiment process contains two phases, the training phase and the testing phase. During training, each transmitted signal $\mathbf{s}$ is generated from the corresponding set of constellations (e.g., BPSK, 16QAM or 64QAM) by following a random normal distribution. The MIMO channel $\mathbf{H}$ is randomly generated from an independent identically distributed (i.i.d.) Gaussian distribution with mean zero and unit variance and assumed to be exactly known at the receiver. Also, the channel noise $\mathbf{n}$ is sampled from a zero-mean i.i.d. normal distribution with a variance that is obtained according to the definition $\text{SNR(dB)} = 10\log(KE_x/\sigma^2)$. Besides, we train AMIC-Net for 10000 iterations with batch size of 2000 for each iteration under BPSK modulation and 16000 iterations with batch size of 500 for each iteration under 16-QAM or 64-QAM modulation. For each training batch, the SNR is chosen randomly from a uniform distribution on $\mathcal{U}(0\ \text{dB} - 16\ \text{dB})$. In order to train the network well, we employ an ADAM optimizer [28] with an initial learning rate of 0.0001 and an exponential decay of 0.97 per 500 training iterations, and the training datasets contain 200000 samples. On the other hand, we evaluate the performance of the well-trained network in the testing phase using the testing datasets with 20000 samples. This training and testing procedure conforms to the vast majority of experimental setups in the relevant literature [20]–[23].

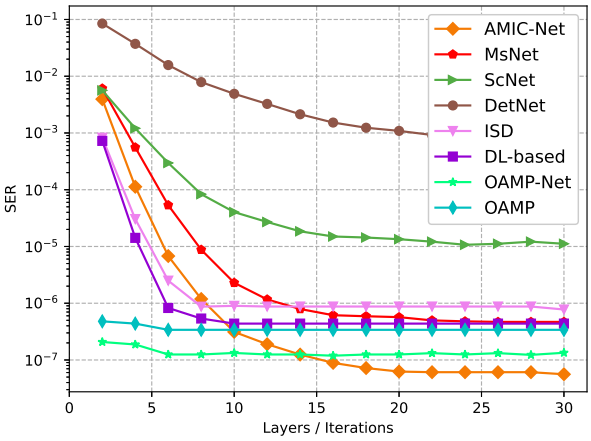

Fig. 6. Symbol erro rate (SER) vs. Layers or Iterations at 12 dB in a (16, 128) system (i.e., $K = 16$, $M = 128$) using 16-QAM modulation.

B. Detection Performance

Fig. 6 illustrates the symbol error rate (SER) performance with different numbers of Layers (Iterations) at 12 dB. We consider a (16, 128) system (i.e., K=16, M=128), and 16-QAM modulation is employed. From Fig. 6, ISD and DL-based can converge at about 8 iterations, OAMP and OAMP-Net converge at about 6 iterations, DetNet, ScNet, MsNet and the proposed AMIC-Net converge at about 25 layers. Although OAMP, OAMP-Net, etc., only require a few layers to achieve respectable performance, their detection performance remains stable as the number of layers grows. However, the proposed AMIC-Net can achieve a lower SER than OAMP and OAMP-Net by deepening the number of layers up to 14 and above; this is attributed to the high level of nonlinearity and flexibility of the data-driven approach, which endows the AMIC-Net with higher performance bounds. Layers or iterations analysed above are adopted in the subsequent simulation experiments.

1) Comparison between Different Activation Functions.

Figs. 7 and 8 show the SER performance of the proposed AMIC-Net with various activation functions, such as sigS$(\cdot)$, SoftSum$(\cdot)$ and SoftS$(\cdot)$, for BPSK modulation and 64-QAM modulation, respectively. As can be seen, at 10^{-5} SER, the AMIC-Net with SoftS$(\cdot)$ function has gain margin of about 0.3 dB and 0.6 dB over the AMIC-Net with SoftSum$(\cdot)$ function at BPSK modulation and 64-QAM modulation, respectively, which reveals that learnable parameters can be added to the activation function to further increase detection accuracy. Moreover, we can also observe that the AMIC-Net with SoftS$(\cdot)$ function has a slight performance gain compared to the AMIC-Net with sigS$(\cdot)$ function under BPSK modulation, especially in low and medium SNR regions. However, under 64-QAM modulation, the AMIC-Net with SoftS$(\cdot)$ function significantly outperforms the AMIC-Net with sigS$(\cdot)$ function by about 2.5 dB at 10^{-4} SER. This implies that

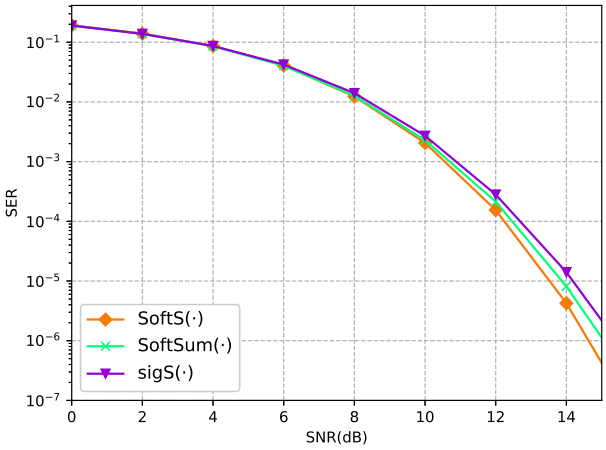

Fig. 7. SER performance of the proposed AMIC-Net with various activation function in a (32, 64) system (i.e., $K = 32$, $M = 64$) using BPSK modulation.

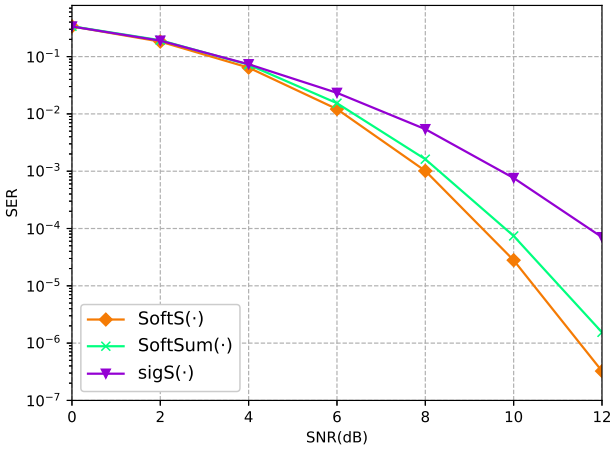

Fig. 8. SER performance of the proposed AMIC-Net with various activation function in a (32, 128) system (i.e., $K = 32$, $M = 128$) using 64-QAM modulation.

our designed activation function is far superior in complex scenarios with high-order modulation. It is mainly due to the non-saturated nature of the SoftS$(\cdot)$ function and its flatter curve compared to the sigS$(\cdot)$ function that allows the AMIC-Net with SoftS$(\cdot)$ function to avoid vanishing gradient and to learn more efficiently in the training phase, thus making it possible to solve the symbol detection difficulties for high-order modulation.

2) Detection Performance Under BPSK Modulation.

Fig. 9 compares the SER performance of the proposed AMIC-Net with that of the MMSE, ISD, DL-based, OAMP, OAMP-Net, DetNet, ScNet and MsNet with different system configurations under BPSK modulation. It can be seen that when the (8, 64) system configuration is employed, all the considered detectors (except for the DetNet, OAMP-Net and AMIC-Net) have similar performance in terms of SER; this is due to the fact that detectors under such conditions can take full advantage of the channel hardening phenomenon [29], leading to near optimal performance. Nevertheless, the proposed AMIC-Net shows close performance to OAMP-Net and obviously outperforms ISD detector by about 0.8 dB at 10^{-5} SER. When the number of transmit antennas increases to 32, our proposed AMIC-Net brings great performance improvement for ISD detector and has significant advantages over other detectors (except for the OAMP-Net); for example, it provides performance gains of about 1 dB at 10^{-5} SER and 2.7 dB at 10^{-4} SER compared to MsNet and MMSE detectors, respectively.

3) Detection Performance Under High-order QAM Modulation.

In Figs. 10 and 11, we investigate the performance of the AMIC-Net, MsNet, ScNet, OAMP-Net, DL-based, ISD, OAMP and MMSE detector under 16-QAM and 64-QAM modulation, respectively, where two different system configurations are considered, such as (16, 128) and (32, 128). From Fig. 10, we can observe that when the system configuration is (16, 128), the SER performance of all the considered detectors (except the MMSE detector) is comparable and exceeds the MMSE detector in the low SNR region. However, when the number of transmit antennas increases to two times, our proposed AMIC-Net shows superior performance and outperforms MsNet and DL-based by 0.5 dB and 1.2 dB at 10^{-5} SER, respectively. It is clear that the AMIC-Net and MsNet suffer a slight performance loss as the number of transmit antennas increases due to their staircase activation functions designed to accommodate high-order modulation schemes. As shown in Fig. 11, the detection performance of MsNet is badly degraded, even worse than that of the DL-based and OAMP detector. Nevertheless, the proposed AMIC-Net still significantly outperforms other detectors (except for the OAMP-Net). Specifically, its performance exceeds DL-based by 0.8 dB and 1.5 dB at 10^{-5} SER for 16 and 32 transmit antennas, respectively. In addition, compared to the 16-QAM modulation scheme, the AMIC-Net has almost no degradation in detection accuracy, which is attributed to the design of SoftS$(\cdot)$ function that allows AMIC-Net network to learn more efficiently in the training process, thus overcoming the difficulties of symbol detection due to the increase in the order of higher modulation. In general terms, we can also observe from these two sets of graphs that the proposed AMIC-Net greatly enhances the performance of traditional ISD detector and has almost the same detection accuracy as OAMP-Net. Furthermore, compared with ISD and DL-based, the AMIC-Net offers a broader choice of antenna ranges for massive MIMO due to its detection performance with lower sensitivity to system size than ISD and DL-based.

C. Complexity Analysis

Despite the superior and stable detection performance of OAMP and OAMP-Net, they require matrix inversion operations similar to MMSE at each iteration step, resulting in a computational complexity of $\mathcal{O}(LK^3)$, which is at least 10 times more than that of the other detectors mentioned

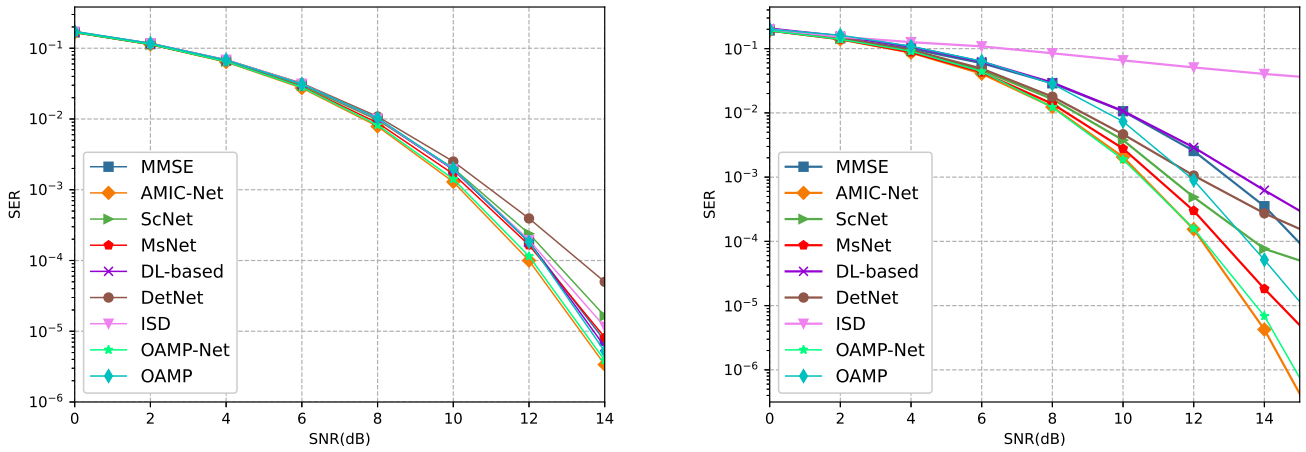

(a) $K = 8$, $M = 64$ (b) $K = 32$, $M = 64$

Fig. 9. SER performance comparison of different detection schemes under BPSK modulation with two system configurations.

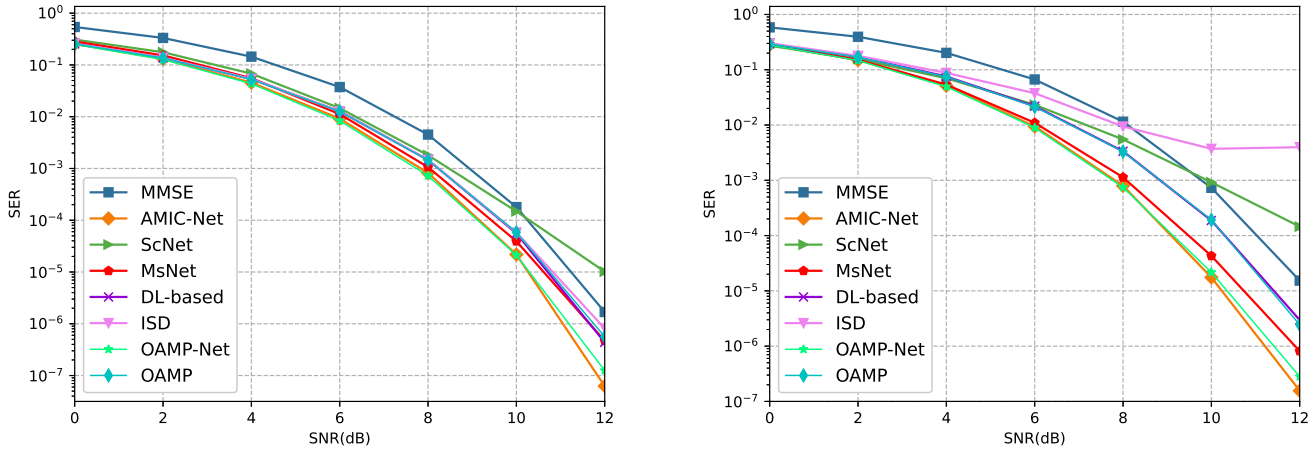

(a) $K = 16$, $M = 128$ (b) $K = 32$, $M = 128$

Fig. 10. SER performance comparison of different detection schemes under 16-QAM modulation with two system configurations.

TABLE II
COMPUTATIONAL COMPLEXITY COMPARISON.

$K \times M$ channel	BPSK	16-QAM
DetNet	$2K^2M + 2KM - K^2 - K + L(14K^2 + 3K)$	$16K^2M + 8KM - 4K^2 - 2K + L(56K^2 + 6K)$
ScNet	$2K^2M + 2KM - K^2 - K + L(2K^2 + 7K)$	$16K^2M + 8KM - 4K^2 - 2K + L(8K^2 + 14K)$
MsNet	$2K^2M + 2KM - K^2 - K + L(2K^2 + 8K)$	$16K^2M + 8KM - 4K^2 - 2K + L(8K^2 + 16K)$
ISD	$2K^2M + 2KM - K^2 - 2K + L(2K^2 + 3K)$	$16K^2M + 8KM - 4K^2 - 4K + L(8K^2 + 6K)$
DL-based	$2K^2M + 2KM - K^2 - 2K + L(2K^2 + 6K)$	$16K^2M + 8KM - 4K^2 - 4K + L(16K^2 + 12K)$
AMIC-Net	$2K^2M + 2KM - K^2 - 2K + L(2K^2 + 13K)$	$16K^2M + 8KM - 4K^2 - 4K + L(8K^2 + 26K)$

here except for the DetNet detector. In Table II, we broadly estimated the computational complexity of the DetNet, ScNet, MsNet, ISD, DL-based, and AMIC-Net based on the number of multiplicative and additive operations. First of all, for BPSK modulation, the overall computational complexity consists of two main parts: 1) Initialization step, i.e., the computation of $\mathbf{H}^T\mathbf{y}$, $\mathbf{H}^T\mathbf{H}$, $\mathbf{D}^{-1}$ and initial solution which involves the multiplication of the diagonal matrix $\mathbf{D}^{-1}$ with $\mathbf{H}^T\mathbf{y}$, requiring $K(2M-1)$, $K^2(2M-1)$, K and $2K$ operations respectively. 2) L-iteration process, for our proposed AMIC-Net, since the

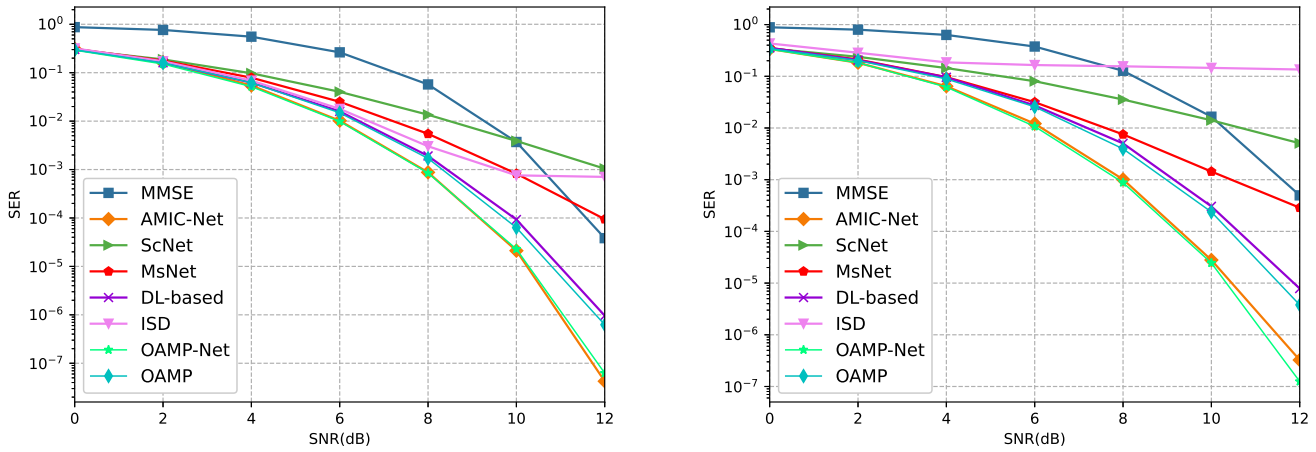

(a) $K = 16$, $M = 128$ (b) $K = 32$, $M = 128$

Fig. 11. SER performance comparison of different detection schemes under 64-QAM modulation with two system configurations.

sparse matrix $\mathbf{P}$ has only $2K$ non-zero entries, the Hadamard product of $\mathbf{P}$ with weight $\mathbf{W}$ requires $2K$ operations. Similarly, calculating the multiplication of the sparse weight matrix $\mathbf{W}$ with the concat requires $5K$ operations. Thus, the complexity required for one iteration contains matrix-vector multiplication, vector-vector addition and other basic operations is $2K^2 + 13K$ operations. Plus the computational complexity of initialization step, the total complexity of the AMIC-Net is given as $2K^2M + 2KM - K^2 + 2K + L(2K^2 + 13K)$. The complexity comparison is presented in Table II.

From Table II, the AMIC-Net requires $8K^2 - 14K$ fewer operations in each iteration than the DL-based for 16-QAM, which is attributed to the fact that the DL-based adds two layers in the network structure to obtain lower SER. However, the AMIC-Net has more layers than the DL-based, so the overall complexity of the AMIC-Net is approximately the same as that of DL-based. In addition, regardless of BPSK modulation or 16QAM modulation, the proposed AMIC-Net has the same coefficients at K^2 and K^2M as other considered detectors (except the DetNet and DL-based), which indicates that the AMIC-Net has comparable computational complexity with these detectors for the same iterations. Therefore, the additional complexity of the AMIC-Net mainly comes from the number of iterations. Note that the complexity of the AMIC-Net is much lower than that of DetNet. In general, our proposed AMIC-Net shows superior detection performance with low complexity.

Fig. 12 shows the variation of the number of learnable parameters with the number of network layers. When the layer dimension, which determines the number of neurons, is fixed, the model size is determined by the number of learnable parameters and the number of network layers. As a result, it can be seen that model-driven DL-based and OAMP-Net require very little memory space and training time to build the models due to the few learnable parameters, but it also limits their ability to go for unprecedented performance improvements and solve complex situations for massive MIMO. However,

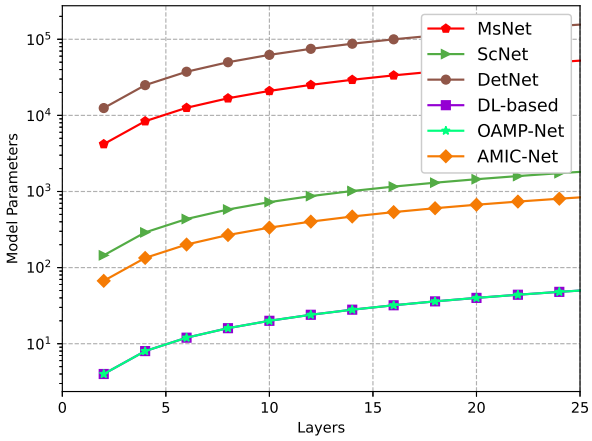

Fig. 12. Number of parameters at different layers.

the proposed AMIC-Net with sufficient learnable parameters can achieve promising performance with much less training time and memory consumption than DetNet.

V. Conclusion

In this letter, we proposed an efficient data-driven AMIC-Net for massive MIMO detection. AMIC-Net is obtained by unfolding the iterative AMIC and adopting a sparsely connected approach. Moreover, in order to improve detection performance under higher-order modulation, we proposed a novel SoftS activation function, which is designed by building a staircase function based on the softsign activation function and adding additional learnable parameters. Numerical results demonstrate that the proposed AMIC-Net has almost the same detection accuracy as OAMP-Net, but with at least 10 times lower computational complexity. Furthermore,

AMIC-Net brings significant performance gain to ISD detector with various massive antenna settings and outperforms the existing detectors, including data-driven DetNet, ScNet, MsNet, model-driven DL-based, and conventional algorithms MMSE, ISD and OAMP detectors, in terms of computational complexity and detection performance, especially in high-order QAM modulation scenarios.

REFERENCES

[1] B. Panzner, W. Zirwas, S. Dierks, M. Lauridsen, and D. Miao, "Deployment and implementation strategies for massive mimo in 5g," in *Proc. IEEE GLOBECOM Workshops*, 2014.

[2] H. Han *et al.*, "A gcica grant-free random access scheme for m2m communications in crowded massive mimo systems," *IEEE Internet of Things J.*, vol. 9, no. 8, pp. 6032–6046, 2022.

[3] H. Han, W. Zhai, Y. Li, W. Lu, and J. Zhao, "A novel random access scheme for m2m communication in crowded asynchronous massive mimo systems," *IET Commun.*, 2021.

[4] E. G. Larsson, O. Edfors, F. Tufvesson, and T. L. Marzetta, "Massive mimo for next generation wireless systems," *IEEE Commun. Mag.*, vol. 52, no. 2, pp. 186–195, Feb. 2014.

[5] B. Wang, F. Gao, S. Jin, H. Lin, and G. Y. Li, "Spatial-and frequency wide band effects in millimeter-wave massive mimo systems," *IEEE Trans. Signal Process.*, vol. 66, no. 13, pp. 3393–3406, Jul. 2018.

[6] T. Kailath, H. Vikalo, and B. Hassibi, "Mimo receive algorithms," in *Space-Time Wireless Systems: From Array Process. to MIMO Communications*, vol. 3, New York, NY, USA: Cambridge Univ. Press, 2005.

[7] F. Rusek *et al.*, "Scaling up mimo: Opportunities and challenges with very large arrays," *IEEE Signal Process. Mag.*, vol. 30, no. 1, pp. 40–60, Jan. 2013.

[8] Z. Guo and P. Nilsson, "Algorithm and implementation of the k-best sphere decoding for mimo detection," vol. 24, no. 3, pp. 491–503, 2006.

[9] Z. Q. Luo, W. K. Ma, A. M. So, Y. Ye, and S. Zhang, "Semidefinite relaxation of quadratic optimization problems," *IEEE Signal Process. Mag.*, vol. 27, no. 3, pp. 20–34, 2010.

[10] C. Jeon, R. Ghods, A. Maleki, and C.Studer, "Optimality of large mimo detection via approximate message passing," *Proc. IEEE ISIT*, 2015.

[11] J. Ma and L. Ping, "Orthogonal amp," *IEEE Access*, vol. 5, no. 14, pp. 2020–2033, Jan. 2017.

[12] S. Dorner, S. Cammerer, J. Hoydis, and S. T. Brink, "Deep learning based communication over the air," *IEEE J. Sel. Topics Signal Process.*, vol. 12, no. 1, pp. 132–143, Feb. 2018.

[13] H. H. *et al.*, "Model-driven deep learning for physical layer communications," *IEEE Wireless Commun.*, vol. 26, no. 5, pp. 77–83, Oct. 2019.

[14] Z. Qin, H. Ye, G. Y. Li, and B.-H.-F. Juang, "Deep learning in physical layer communications," *IEEE Wireless Commun.*, vol. 26, no. 2, pp. 93–99, Apr. 2019.

[15] Y. Wei *et al.*, "Learned conjugate gradient descent network for massive mimo detection," *IEEE Trans. Signal Process.*, vol. 68, pp. 6336–6349, 2020.

[16] J. Liao, J. Zhao, F. Gao, and G. Y. Li, "A model-driven deep learning method for massive mimo detection," *IEEE Commun. Lett.*, vol. 24, no. 8, pp. 1724–1728, 2020.

[17] H. He, C.-K. Wen, S. Jin, and G. Y. Li, "A model-driven deep learning network for mimo detection," in *Proc. IEEE GlobalSIP*, 2018.

[18] B. Yin, M. Wu, J. R. Cavallaro, and C. Studer, "Conjugate gradient-based soft-output detection and precoding in massive mimo systems," in *Proc. IEEE GLOBECOM*, 2014.

[19] M. Mandloi and V. Bhatia, "Low-complexity near-optimal iterative sequential detection for uplink massive mimo systems," *IEEE Commun. Lett.*, vol. 21, no. 3, pp. 568–571, Oct. 2017.

[20] N. Samuel, T. Diskin, and A. Wiesel, "Deep MIMO detection," in *Proc. IEEE SPAWC*, Jul. 2017.

[21] N. Samuel, T. Diskin, and A. Wiesel, "Learning to detect," *IEEE Trans. Signal Process.*, vol. 67, no. 10, pp. 2554–2564, 2019.

[22] G. Gao, C. Dong, and K. Niu, "Sparsely connected neural network for massive mimo detection," in *Proc. IEEE ICCC*, 2018.

[23] Y. Yu, J. Wang, and L. Guo, "Multisegment mapping network for massive mimo detection," *Int. J. Antennas and Propag.*, 2021.

[24] Y. LeCun, Y. Bengio, and G. Hinton, "Deep learning," *Nature*, vol. 521, no. 7553, pp. 436–444, 2015.

[25] J. Wu, Z. Wang, and X. Li, *Efficient solution and parallel computation of sparse linear systems of equations*. Changsha, China: Hunan Science and Technology Press, 2004.

[26] L. Dai *et al.*, "Low-complexity soft-output signal detection based on gauss-seidel method for uplink multiuser large-scale mimo systems," *IEEE Trans. Veh. Technol.*, vol. 64, no. 10, pp. 4839–4845, Oct. 2015.

[27] M. Abadi *et al.*, "Tensorflow: A system for large-scale machine learning," in *Proc. OSDI*, 2016.

[28] D. P. Kingma and J. Ba, "Adam: A method for stochastic optimization," in *Proc. ICLR*, 2014.

[29] B. M. Hochwald, T. L. Marzetta, and V. Tarokh, "Multiple-antenna channel hardening and its implications for rate feedback and scheduling," *IEEE Trans. Inf. Theory*, vol. 50, no. 9, pp. 1893–1909, 2004.

Yongzhi Yu received the B.S. degree in Communication Engineering from Harbin Engineering University, Harbin, China, in 2003, and the M.S. and Ph.D. degrees in Signal and Information Processing from Harbin Engineering University, Harbin, China, in 2006 and 2009, respectively. In September 2003, he joined the Faculty of Harbin Engineering University, Harbin, China, where he is currently a Lecture in the College of Information and Communication Engineering. During 2011, he visited University of Glasgow, Glasgow, UK, as a Visiting Scholar. His research interests include digital communications, radar signal processing, and coding techniques applied to wireless systems.

Jie Ying received the B.S. degree in Communication Engineering from Southwest Petroleum University, Chengdu, China, in 2020. He is currently pursuing the graduation degree in Electronic Information with the College of Information and Communication Engineering, Harbin Engineering University, Harbin, China. His research interests include signal detection for massive MIMO systems, communication signal processing and deep learning.

Ping Wang is an Associate Professor at the Department of Electrical Engineering and Computer Science, York University, and a Tier 2 York Research Chair. Prior to that, she worked with Nanyang Technological University, Singapore, from 2008 to 2018. Her research interests are mainly in the area of wireless communication networks, cloud computing and Internet of things with the recent focus on integrating artificial intelligence (AI) techniques into communications networks. She has published more than 250 papers/conference proceedings papers. Her scholarly works have been widely disseminated through top-ranked IEEE journals/conferences and received the Best Paper Awards from IEEE Wireless Communications and Networking Conference (WCNC) in 2022, 2020 and 2012, from IEEE Communication Society: Green Communications & Computing Technical Committee in 2018, and from IEEE International Conference on Communications (ICC) in 2007. Her work received 21,000+ citations with an H-index of 70 (Google Scholar). She is an IEEE Fellow and a Distinguished Lecturer of the IEEE Vehicular Technology Society.

Limin Guo received the B.S. degree in Communication Engineering from Harbin Engineering University, Harbin, China, in 2000, and the M.S. and Ph.D. degrees in Communication and Information system from Harbin Engineering University, Harbin, China, in 2005 and 2009, respectively. In September 2000, he joined the Faculty of Harbin Engineering University, Harbin, China, where he is currently an Associate Professor in the College of Information and Communication Engineering. He is mainly engaged in broadband signal detection, processing and recognition, image processing, control and simulation research.